

Electronic Supplementary Material

Effective and selective adsorption of uranyl ions by porous polyethylenimine-functionalized carboxylated chitosan/oxidized activated charcoal composite

Juan Shen (✉)^{1,2}, Fang Cao¹, Siqi Liu¹, Congjun Wang¹, Rigui Chen¹, Ke Chen¹

¹ School of Materials Science and Engineering, Southwest University of Science and Technology, Mianyang 621010, China

² State Key Laboratory of Environmental-friendly Energy Materials, Southwest University of Science and Technology, Mianyang 621010, China

E-mail: sj-shenjuan@163.com

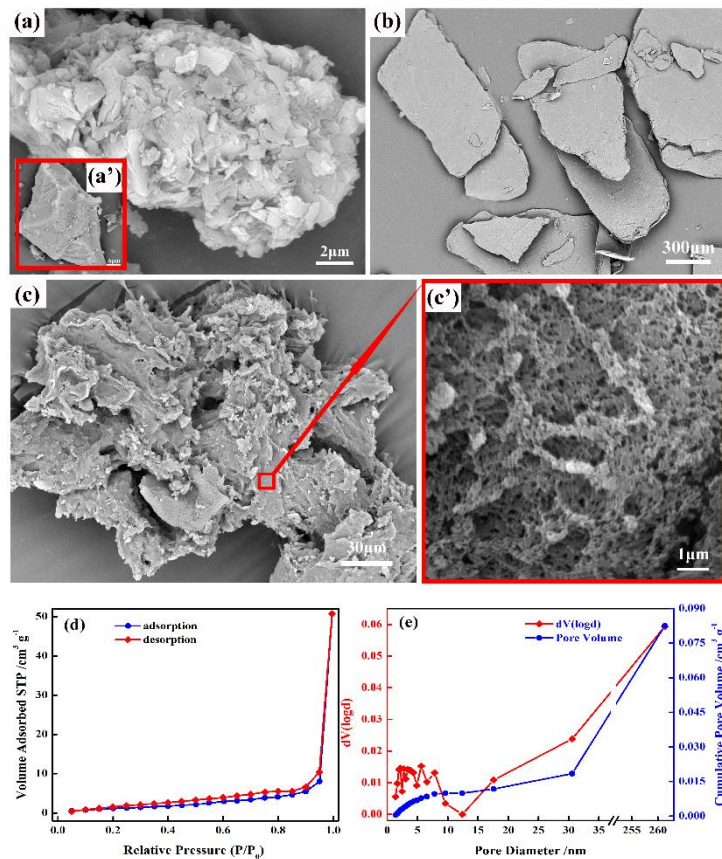


Fig. S1 (a) The surface morphology of the oxidized activated charcoal. (a') The

surface morphology of the activated charcoal. (b) The surface morphology of the carboxylated chitosan. (c) The surface morphology of the PCO. (c') The high-magnification surface morphology of the PCO. (e) The Nitrogen adsorption and desorption isotherms of PCO. (e) The corresponding BJH pore size distribution of PCO.

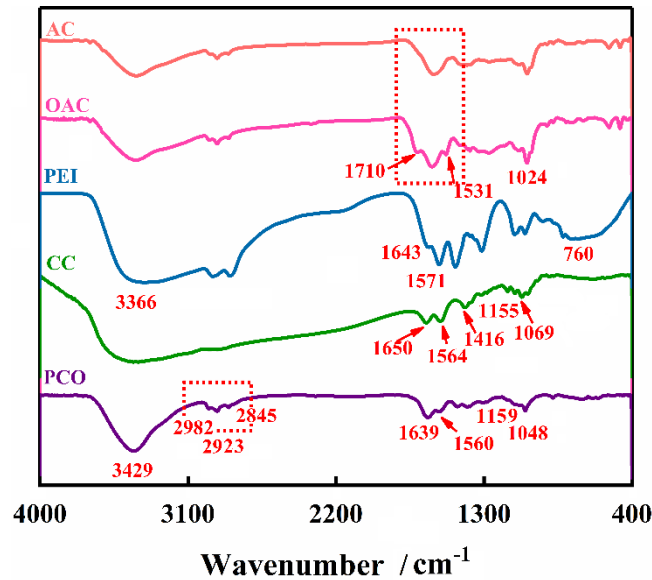


Fig. S2 FT-IR spectra of AC, OAC, PEI, CC, PCO and PCO after uranyl ions adsorption.

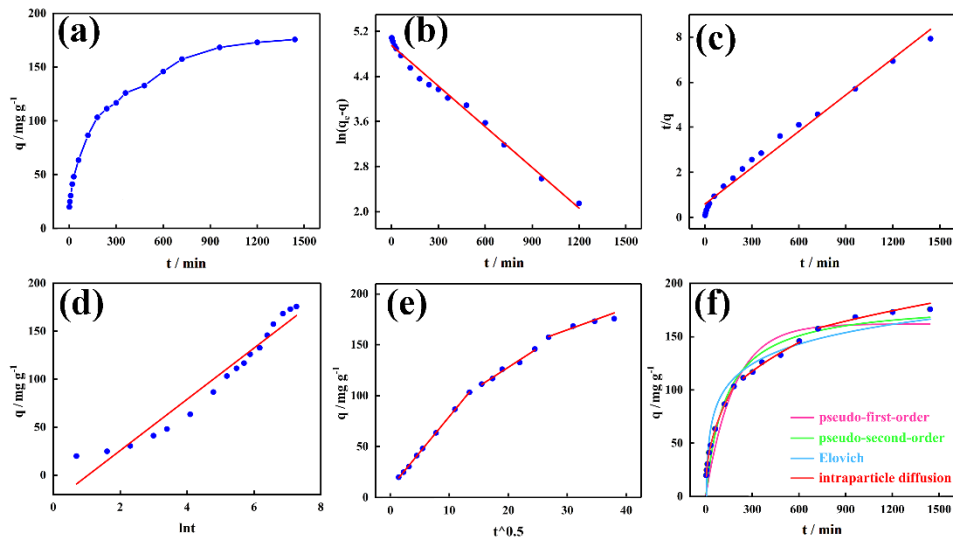


Fig. S3 (a) Effect of contact time on the adsorption capacities of PCO. ($C_0=100 \text{ mg L}^{-1}$, $\text{pH}=4$, $m=0.01 \text{ g}$, $V=20 \text{ mL}$, and $T=298 \text{ K}$) (b) linear fitting curve of

pseudo-first-order kinetic model. (c) linear fitting curve of pseudo-second-order kinetic model. (d) linear fitting curve of the Elovich kinetic model. (e) linear fitting curve of intraparticle diffusion kinetic model. (f) nonlinear fitting curves of four kinetic models.

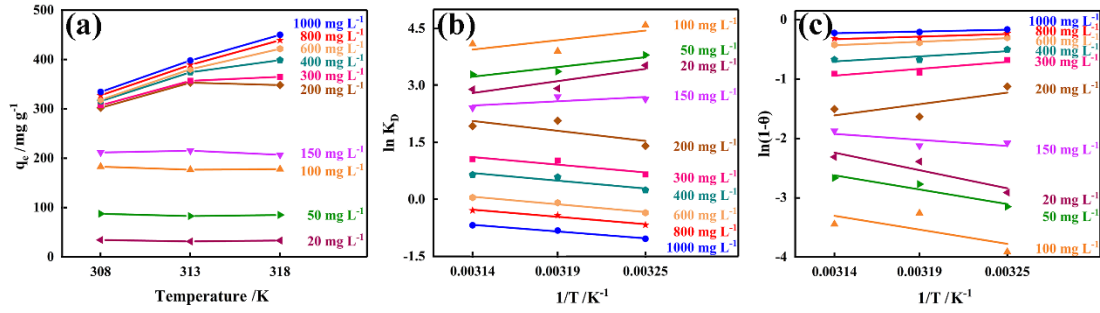


Fig. S4 (a) Effect of temperature on the adsorption capacities of PCO under different initial uranyl ion concentration. (pH=4, m=0.01 g, V=20 mL, and t=24 h) (b) Relationship between $1/T$ and $\ln K_D$. (c) Relationship between $1/T$ and $\ln(1-\theta)$.

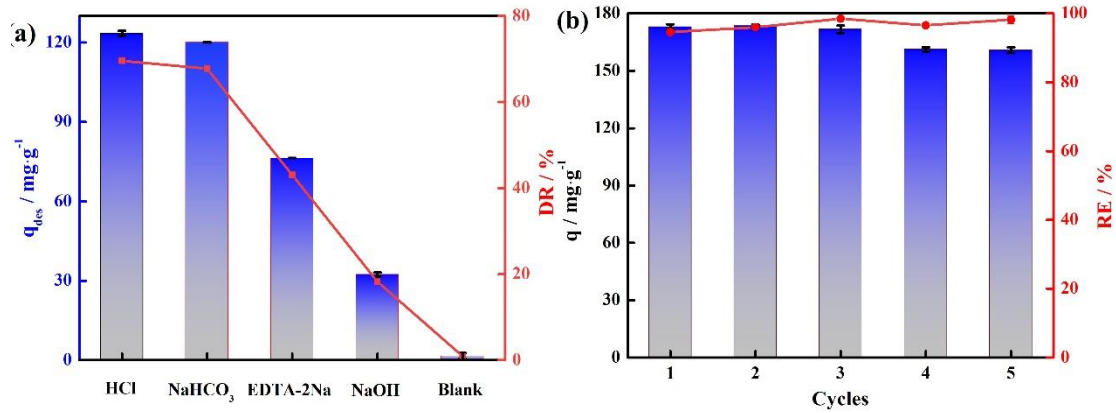


Fig. S5 (a) Effect of different desorbents on the desorption capacity and desorption rate of PCO after adsorbed uranyl ions. ($C_{desorbents}=0.1$ mol L⁻¹, m=0.025 g, V=50 mL, T=318 K, and t=24 h) (b) Effect of cycles number on the adsorption capacity and removal efficiency of PCO. ($C_{NaHCO_3}=0.5$ mol L⁻¹, m=0.025 g, V=50 mL, T=318 K, and t=24 h)

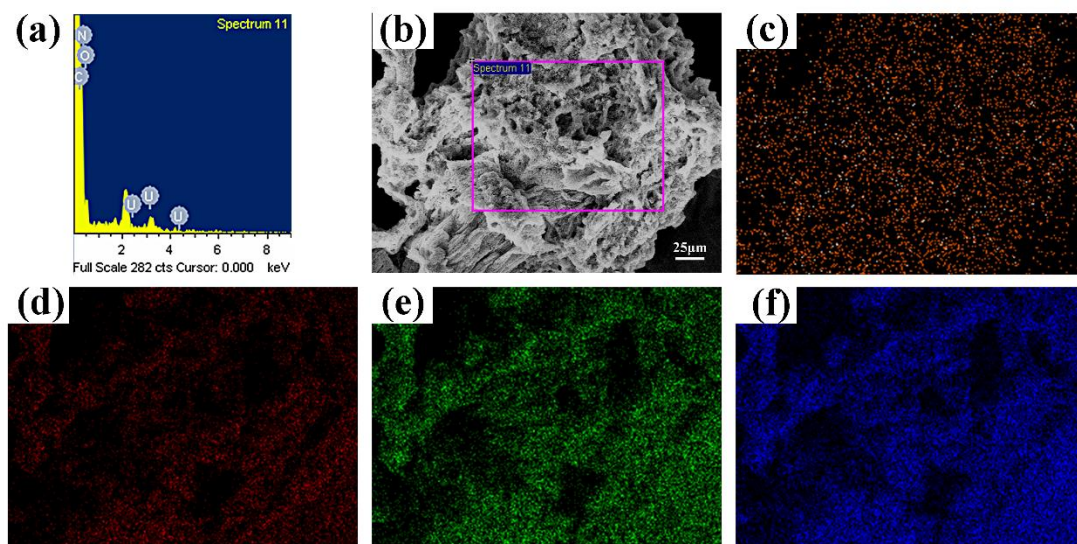


Fig. S6 (a) EDX spectrum of PCO after uranyl ions adsorption. (b) The surface morphology of the PCO after uranyl ions adsorption. (c-f) EDX elemental mapping images of PCO after uranyl ions adsorption: (c) U; (d) O; (e) N; (f) C.

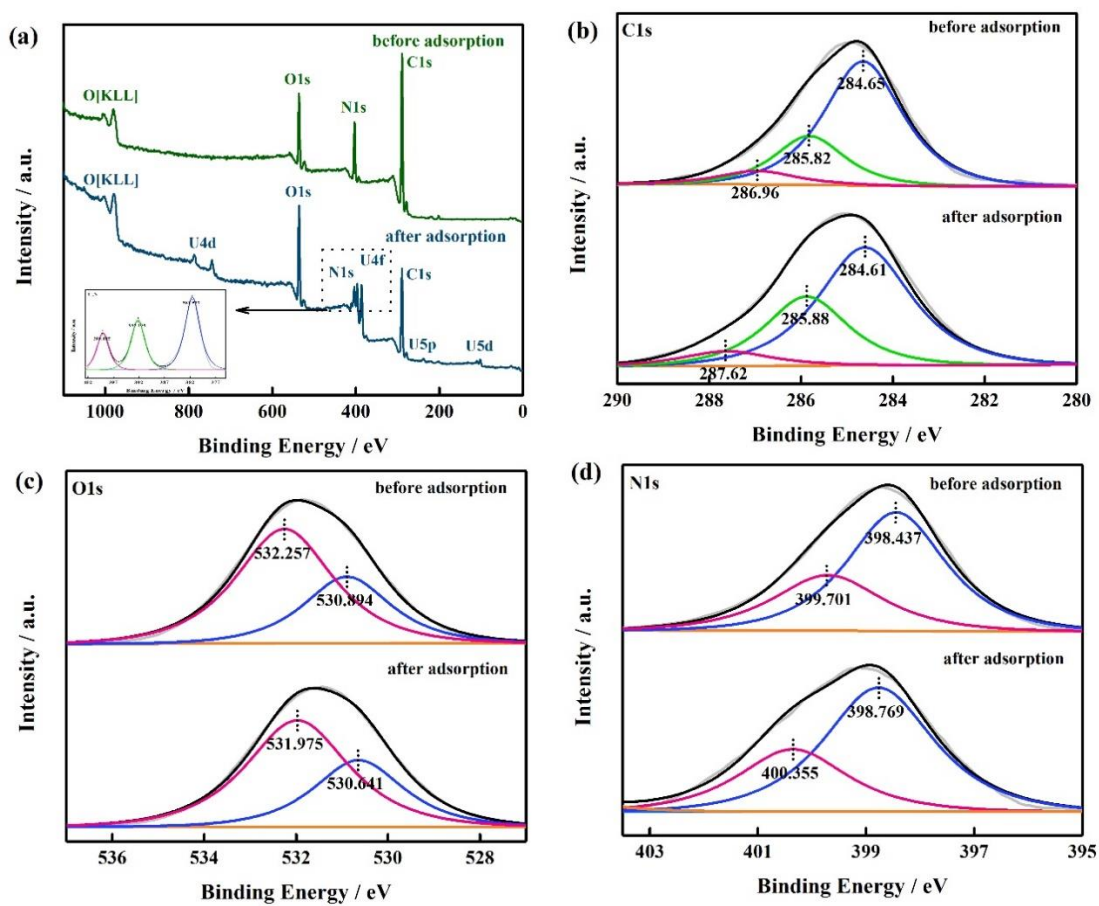


Fig S7 (a) Typical XPS survey of PCO before and after uranyl ions adsorption. (b) High resolution of C 1s spectra. (c) High resolution of O 1s spectra. (d) High resolution of N 1s spectra.

Table S1. The fitting parameters of pseudo-first-order, pseudo-second-order, the Elovich and intraparticle diffusion kinetic models.

Type		Linear model
pseudo-first-order	k_1 (min^{-1})	0.0024
	q_e (mg g^{-1})	141.5566
	R_{adj}^2	0.9886
pseudo-second-order	k_2 ($\text{g mg}^{-1} \text{min}^{-1}$)	2.8944×10^{-5}
	q_e (mg g^{-1})	185.8736
	R_{adj}^2	0.9838
Elovich	α ($\text{mg g}^{-1} \text{min}^{-1}$)	9.4694
	β (g mg^{-1})	0.0375
	R_{adj}^2	0.9424
intraparticle diffusion	k_i ($\text{mg g}^{-1} \text{min}^{-1/2}$)	$k_{d1}=9.4025; k_{d2}=3.7447; k_{d3}=2.0925$
	C	$C_1=7.0185; C_2=53.0302; C_3=101.9038$
	R_{adj}^2	$R_{1\text{adj}}^2=0.9996; R_{2\text{adj}}^2=0.9789; R_{3\text{adj}}^2=0.9746$

Table S2. The fitting parameters of the Langmuir, the Freundlich, the D-R and the Temkin isotherm models.

Type			308.15K	313.15K	318.15K
Langmuir	Linear	q_{\max} (mg g ⁻¹)	334.4481	400.0000	456.6210
		K_L (L mg ⁻¹)	0.1047	0.0780	0.0485
		R_{adj}^2	0.9995	0.9996	0.9990
	Nonlinear	q_{\max} (mg g ⁻¹)	337.6901	393.9819	476.5793
		K_L (L mg ⁻¹)	0.3063	0.1203	0.1285
		R_{adj}^2	0.8969	0.9485	0.9388
Freundlich	Linear	K_F (L mg ⁻¹)	80.4230	66.9021	65.3522
		n	4.1386	3.2425	3.0714
		R_{adj}^2	0.6762	0.6982	0.7441
	Nonlinear	K_F (L mg ⁻¹)	121.4743	122.3360	113.2517
		n	6.1687	5.2460	4.5839
		R_{adj}^2	0.7977	0.7857	0.8619
D-R	Linear	q_{\max} (mg g ⁻¹)	297.7100	341.4871	363.3730
		β	6.9681×10^{-7}	1.7304×10^{-6}	1.8278×10^{-6}
		R_{adj}^2	0.8980	0.9338	0.8723
	Nonlinear	q_{\max} (mg g ⁻¹)	303.4865	379.8496	413.4756
		β	7.0294×10^{-7}	1.8521×10^{-5}	3.8078×10^{-5}
		R_{adj}^2	0.8443	0.7384	0.7645
Temkin	Linear	K_T (L g ⁻¹)	10.8009	2.9857	1.9535
		A	38.9850	55.5452	64.0029
		R_{adj}^2	0.8716	0.8881	0.9350
	Nonlinear	K_T (L g ⁻¹)	9.1774×10^5	1.2370×10^6	266.4958
		A	16.2357	19.0924	36.4710
		R_{adj}^2	0.9789	0.9887	0.9922

Table S3. Thermodynamic parameters of PCO on uranyl ions adsorption.

C ₀ (mg L ⁻¹)	ΔH (kJ mol ⁻¹)	ΔS (J mol ⁻¹ K ⁻¹)	ΔG (kJ mol ⁻¹)			S* (J K mol ⁻¹)	E _a (kJ mol ⁻¹)
			288.15K	298.15K	308.15K		
20	-51.7746	-139.4403	-8.8061	-8.1089	-7.4117	1.1767×10 ⁷	-48.9945
50	-41.8160	-104.5673	-9.5936	-9.0707	-8.5479	2.2073×10 ⁵	-39.4882
100	-40.7312	-95.2212	-11.3887	-10.9127	-10.4366	7.6906×10 ⁴	-38.5043
150	-18.3432	-37.0968	-6.9118	-6.7264	-6.5409	74.7359	-16.5066
200	42.8218	151.7755	-3.9478	-4.7067	-5.4656	1.4655×10 ⁻⁶	31.2611
300	33.0127	113.0451	-1.8222	-2.3874	-2.9526	3.0338×10 ⁻⁴	18.9275
400	33.1353	109.9310	-0.7399	-1.2896	-1.8392	2.4742×10 ⁻³	14.0095
600	32.8388	103.8142	0.8485	0.3294	-0.1897	0.0158	9.8350
800	31.1425	95.6553	1.6663	1.1881	0.7098	0.0481	7.1496
1000	28.9992	85.5992	2.6218	2.1938	1.7658	0.1230	4.7877